



<http://www.diva-portal.org>

Preprint

This is the submitted version of a paper published in *Chemical Communications*.

Citation for the original published paper (version of record):

Klechikov, A., Mercier, G., Sharifi, T., Baburin, I A., Seifert, G. et al. (2015)

Hydrogen storage in high surface area graphene scaffolds.

Chemical Communications, 51(83): 15280-15283

<https://doi.org/10.1039/c5cc05474e>

Access to the published version may require subscription.

N.B. When citing this work, cite the original published paper.

Permanent link to this version:

<http://urn.kb.se/resolve?urn=urn:nbn:se:umu:diva-109475>

Hydrogen storage in high surface area graphene scaffolds.

Alexey Klechikov,^a Guillaume Mercier,^a Tiva Sharifi,^a Igor A. Baburin,^b Gotthard Seifert,^b Alexandr V. Talyzin^{a*}

Received 00th January 20xx,
Accepted 00th January 20xx

DOI: 10.1039/x0xx00000x

www.rsc.org/

Using optimized KOH activation procedure we prepared highly porous graphene scaffold materials with SSA values up to 3400 m²/g and pore volume up to 2.2 cm³/g, which are among the highest for carbon materials. Hydrogen uptake of activated graphene samples was evaluated in a broad temperature interval (77–296 K). After additional activation by hydrogen annealing the maximal excess H₂ uptake of 7.5 wt% was obtained at 77 K. A hydrogen storage value as high as 4 wt% was observed already at 193 K (120 bar H₂), temperature of solid CO₂, which can be easily maintained using common industrial refrigeration methods.

Carbon materials with ultra-high surface area are of strong interest for several important energy-related applications: hydrogen storage,¹ supercapacitors,^{2, 3} and batteries.⁴ Therefore, a lot of efforts have been aimed during the past decades on studies of hydrogen storage in various nanostructured porous materials: activated carbons^{5, 6}, carbon nanotubes, templated carbons^{7, 8}, carbide derived carbons⁹ and, more recently, graphene^{10–13}.

Theoretical SSA of ideal single layered graphene is about 2630 m²/g which is often cited as maximal possible value.¹⁴ However, this value is not limiting for materials constructed using highly defect graphene sheets arranged into 3D scaffolds. Recent theoretical modelling results demonstrated that SSA values as high as 5000 m²/g are possible for graphene sheets perforated with small size holes and packed into 3D structure with optimal inter-layer distance of 0.7–1 nm.¹⁵ However, the experimental realization of ordered structures proposed in ref.¹⁵ is hindered by the absence of suitable methods to hold graphene layers separate from each other.

The best of so far known methods to produce highly porous carbon materials is KOH activation, which was extensively studied for a broad range of precursors, including e.g. natural biomaterials and, more recently, reduced graphene oxide (r-GO).^{2, 3, 11} It is known that SSA of carbons produced by KOH activation can be as high as ~3000 m²/g and depends very strongly on the type of the precursor materials.⁴ Using graphene as a precursor can be an advantage due to the more precisely defined shape and possibility to arrange graphene sheets into multilayered structures. Introducing defects e.g. wrinkles, holes and wave-like corrugations

could prevent graphene sheets from aggregation into less porous graphitic structures. Activation of r-GO using annealing with KOH was reported result in samples with 3100 m²/g SSA and with extraordinary high pore volume of 2.14 cm³/g,^{2, 11} which is superior to other carbon materials. Typical pore volumes below 1.4 cm³/g have been reported for carbon materials produced using KOH activation of precursors other than graphene, even for samples with SSA values exceeding 3000 m²/g.⁴ Lower total pore volume of ~1.7 cm³/g was reported also for zeolite-templated carbons with SSA of about 3300 m²/g.¹⁶ Therefore, it is rather interesting to verify hydrogen sorption parameters of KOH activated r-GO samples (a-r-GO) with ultra-high surface area and pore volume.

Rapid thermal exfoliation of graphite oxides results in formation of r-GO consisting of strongly defective single-layered and few-layered graphene sheets.¹⁷ However the SSA of this r-GO is relatively small (up to ~800 m²/g). Much higher SSA of KOH-activated samples has been attributed to the formation of holes in graphene sheets as revealed e.g. by direct electron microscopy observations.^{2, 11, 18} However, hydrogen storage parameters of KOH activated samples with ultra-high SSA of ~3000 m²/g were not reported in these studies.

Recently we re-evaluated hydrogen sorption properties of “graphene” with a broad range of SSA (300–2400 m²/g), including some samples prepared using KOH activation procedure.¹³ However, initially we were not able to reproduce SSA approaching 3000 m²/g following procedure described in the ref.¹¹ Lower SSA values have also been reported in several later studies aimed on KOH activation of graphene-related materials.^{19–21}

Here we report an optimized procedure for KOH activation r-GO which allows to produce reliably and reproducibly materials with SSA up to 3400 m²/g and pore volume 2.2 cm³/g and to evaluate hydrogen storage parameters of activated r-GO (a-r-GO). Therefore, we extended the H₂ uptake vs SSA trends (at 296 K and 77K) to include a broader range of values (300–3300 m²/g).

The r-GO obtained by thermal exfoliation of Hummers graphite oxide was subjected to modified KOH activation tuned to provide samples with ultra-high surface area over 3000 m²/g (see ESI for details). Hydrogen storage parameters were determined in a broad temperature interval using the volumetric method. Several samples were also annealed in-situ under 50 Bar H₂ gas at 673–723 K which resulted in a further increase of H₂ uptakes.

The SSA of activated r-GO (a-r-GO) samples was evaluated using nitrogen adsorption isotherms (Fig. 1a). This isotherm analysed

^a Department of Physics, Umeå University, SE-901 87 Umeå, Sweden

^b Technische Universität Dresden, Theoretische Chemie, Bergstraße 66b, 01062 Dresden

* Corresponding author: alexandr.talyzin@physics.umu.se

† Electronic supplementary information (ESI) available:

: DOI: 10.1039/x0xx00000x

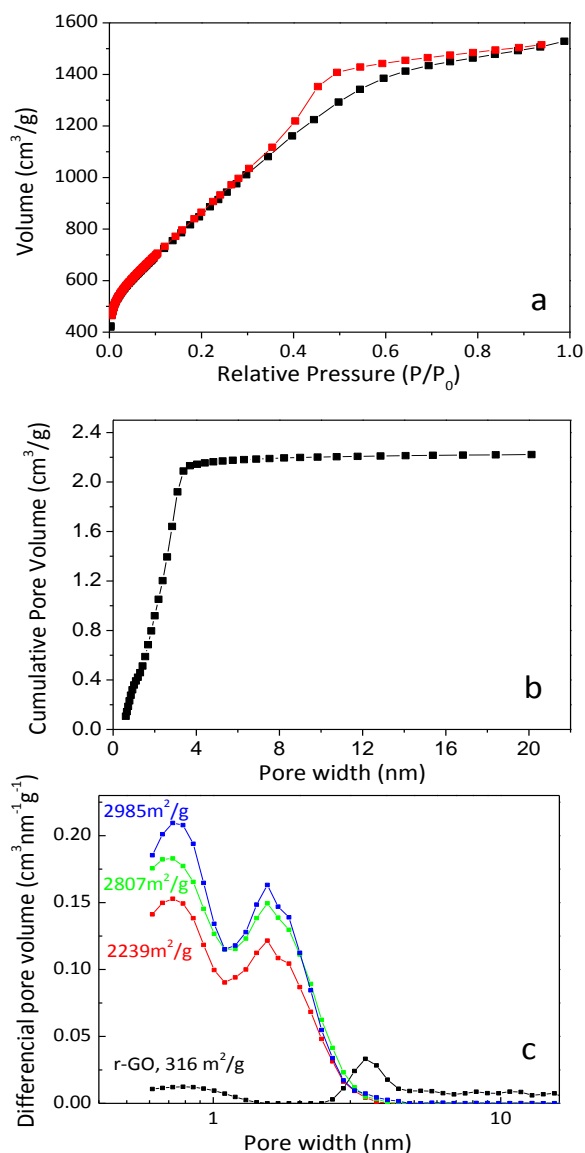


Fig. 1. N₂ adsorption/desorption isotherm for a-r-GO sample (SSA=3300 m²/g) (a) and analysis of isotherms simulated using QSDFT slit pore model: plot of cumulative pore volume (b), pore size distribution (c)

using the BET method provides an SSA value of 3230 m²/g. " The analysis of the isotherm shown in Fig. 1a by the Quenched solid density functional theory (QSDFT) method based on a slit-pore model results in a lower value of 2620 m²/g, while the non local density functional theory (NLDFT) method based on a slit/cylindrical-pore model shows 2660 m²/g. In the following discussions we use SSA values determined by the BET method. Two peaks are typically observed in the pore size distribution plots simulated for a-r-GO using slit pore QSDFT (Fig. 1c), first peak centered approximately at 0.7-0.8 nm and second at ~1.5 nm. The "graphene scaffold" structure created using the KOH activation procedure shows essentially microporous nature in contrast to pristine r-GO obtained by thermal exfoliation (Fig. 1c).

Several a-r-GO samples were additionally annealed in H₂ in order to substitute oxygen containing functional groups with hydrogen. These samples showed a pore size distribution with additional peak corresponding to wider pores with up to ~3 nm (see ESI). Analysis of

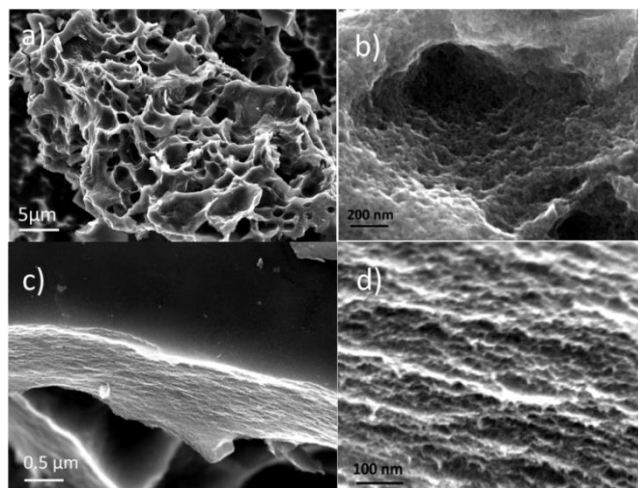


Fig. 2. SEM images recorded from a-r-GO sample with BET surface area of ~3300 m²/g. The images show hierarchical size pore network (a, b) and also some layered structure on broken grain edge (c, d).

pore size distribution for samples with highest SSA shows that a-r-GO is essentially microporous with a size of pores below 3 nm, maximal BET surface area of 3300 m²/g and pore volume up to 2.22 cm³/g (Fig. 1b). The pore volume of a-r-GO samples is superior compared to other nanoporous materials. For example, comparable pore volume of ~2 cm³/g is achieved in Metal Organic Framework (MOF) materials with about twice higher SSA values (~5000-7000 m²/g).^{22, 23} Note that changing the model from slit pore to slit-cylindrical pores results in a rather small change in the pore volume (Fig. 1S in ESI).

The evolution of the sample composition as a result of GO exfoliation and activation was evaluated using XPS (Fig. 2S in ESI). The composition of the precursor GO sample corresponds to C/O=2.63 and increases up to C/O=6.3 after thermal reduction. Annealing of an r-GO/KOH mixture resulted in a further reduction (C/O=24.0), whereas after hydrogen annealing the a-r-GO showed C/O =35.

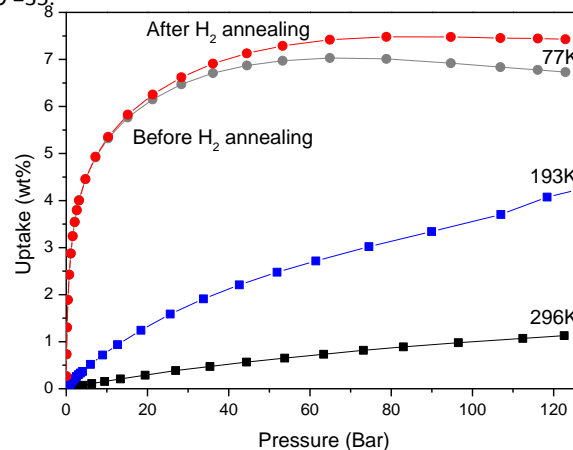


Fig. 3. Excess adsorption isotherms at T=77 K, T=193K and T=296 K for the a-r-GO sample with SSA=3230 m²/g and isotherm recorded at 77K after H₂ annealing.

Both r-GO and a-r-GO samples are non-crystalline solids and show no diffraction peaks. There is also no change in Raman spectra as a

result of activation treatment (Fig. 3S in ESI). Therefore, the microstructure of a-r-GO samples was evaluated also by Scanning Electron Microscopy (SEM) which showed that they consist of grains with a size of up to tens of micrometers (Fig.2).

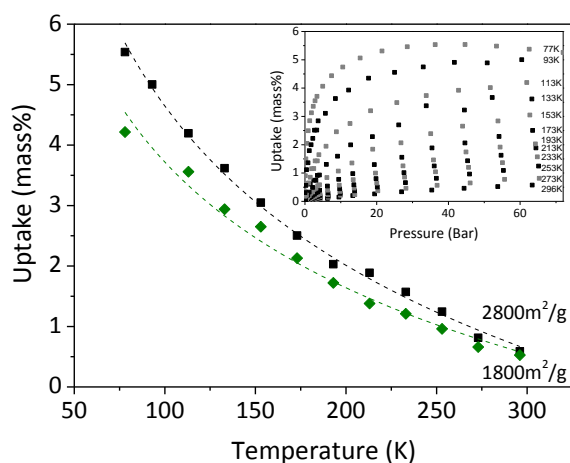


Fig. 4. Temperature dependence of H₂ uptakes for two a-r-GO samples. Inset shows isotherms recorded for a-r-GO sample with 2800 m²/g BET surface area at different temperatures up to the pressure of 65 bar H₂. Isostatic heat of adsorption value of 6.1 kJ/mol was determined for this sample.

The grains exhibit a hierarchically porous structure with typical shapes of observed grains from cheese-like to sponge-like depending on the number of micrometer sized holes (see also ESI). Under higher magnification, smaller pores with a typical size on the scale of few nanometers to tens of nanometers are revealed. A more detailed study showed that broken skeleton-like walls of a-r-GO grains exhibit clearly layered texture (Fig. 2 c,d). The Fig. 3c shows the edge view of a densely packed array of irregularly curved and interconnected layers. The overall structure of our samples can be then described as packs of strongly perforated graphene layers arranged into 3D “scaffolds”.

Hydrogen sorption of a-r-GO samples was evaluated using volumetric method at 77 K and 296 K. An example of H₂ isotherms recorded from high surface area a-r-GO sample (SSA=3230 m²/g) is shown on Fig. 3. The H₂ uptake measured at 77K saturates at ~40 bar (7.04 wt%) whereas at 296 K adsorption is not saturated and reaches 1.13 wt% at 120 bar. The hydrogen uptake was further improved using additional activation by H₂ annealing at 450°C for 2 hours. Remarkably, hydrogen uptakes measured for the annealed sample increased by ~10 % (1.25 wt% at 296 K and 7.48 wt% at 77 K). Nitrogen isotherms were recorded for this sample before H₂ uptake measurements, after H₂ measurements, and finally after H₂ annealing and re-measurement of hydrogen sorption on annealed sample (Sample 2 in the Table 1S) showing only negligible variation. Therefore, the increase of hydrogen sorption as an effect of H₂ annealing should be assigned to a change in the pore size distribution, rather than to an increase of SSA (Fig. 1 c,d). High hydrogen sorption properties of material preserve even after prolonged air exposure and reversible for several cycles (Fig.4S)

The temperature dependence of hydrogen uptake measured for two a-r-GO samples is shown in Fig. 5. The plot includes saturation values for lower temperatures and uptake values specific for 65 bar

H₂ pressure for higher temperature when saturation could not be achieved (inset in Fig.4). Hydrogen uptakes for samples with maximal surface area were also verified at higher H₂ pressure of 120 bar for temperature points of practical interest: 273 K (ice bath) and 193 K (temperature of solid CO₂) (Table 1 in ESI). Remarkably, hydrogen storage with capacity as high as 3.8-4.2 wt% can be achieved already at solid CO₂ temperature. Note that this

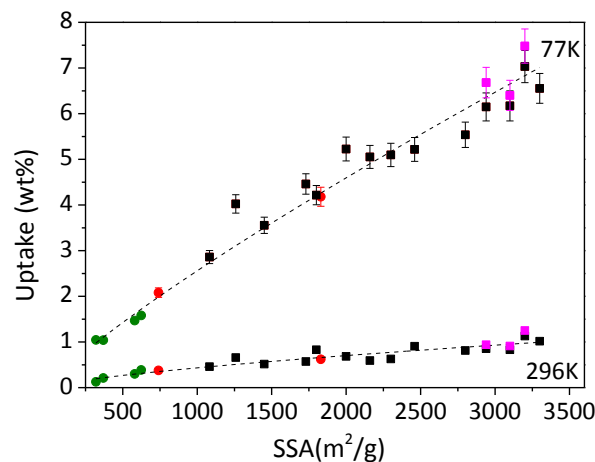


Fig. 5. H₂ uptake (wt%) vs SSA trends evaluated using volumetric method and immersion cell for a-r-GO samples at 296 K (120 bar) and 77 K (saturation value) before (■) and after H₂ annealing (■). The trend is extended showing samples of r-GO (●)¹³ and reference points for Mesoporous Carbon and Activated Carbon (●).

value measured at 120 Bar H₂ is not saturated and can be further improved by pressure increase. Very common industrial refrigeration methods allow maintaining samples at 193K which can be of practical interest for hydrogen storage.

The isosteric heat of adsorption for the sample with maximal storage capacity (Fig.3) was evaluated using four isotherms (following the procedure described in ref²⁴). The value $Q_{st} \sim 6.2-6.4$ kJ/mol can be obtained by rough extrapolation of the adsorption heat to zero uptake (Fig. 5S in ESI). This value is in good agreement with the data reported earlier for high surface area carbon materials (e.g. 6.5 kJ/mol for the sample with SSA of 3591m²/g⁷ and 5.9 kJ/mol for r-GO¹⁰).

Results of hydrogen sorption measurements are summarized in the Fig. 5 which shows SSA vs wt% trends at 77 K and 296 K. It is known that hydrogen uptakes by various carbon materials correlate with BET SSA and shows common trends.^{8, 25,26, 27} Some early studies of hydrogen adsorption by “graphene” reported H₂ uptake values 3-10 fold higher for r-GO samples with relatively small SSA values.^{28,29} However, our experiments demonstrate that H₂ uptakes of “graphene” samples follow standard for all carbon materials trends. Fig. 4 shows updated data which summarize H₂ uptake trends for r-GO and a-r-GO samples for a broad range of SSA values up to ~3300 m²/g. The trends revealed in Fig. 6 demonstrate 0.32 and 2.3 wt% H₂ uptakes per 1000 m²/g for 296 K and 77 K respectively in a good agreement with “Chahine rule”.^{7,30}

An interesting example of deviation from the standard trends is activation of a-r-GO by H₂ annealing. The increase of H₂ uptakes occurs after hydrogen annealing activation without visible change in surface area values or total pore volume, only with some change in

pore size distribution (Fig. 1d). Most likely the effect of H₂ annealing at 723 K is substitution of residual oxygen containing functional groups on the edges of a-r-GO pores with smaller hydrogen atoms. Indeed, Fig. 1d shows broadening of some pores. We suggest that the increase of H₂ uptakes could be explained by contribution of sub-nanometer pores which become accessible for hydrogen as a result of pore broadening by hydrogenation.

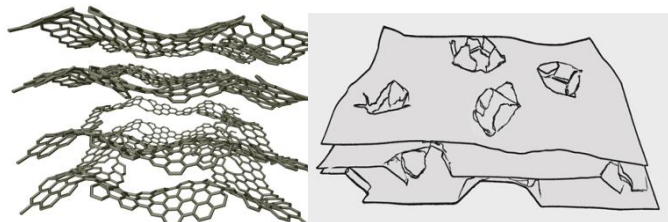


Fig. 6. Schematic representation of possible a-r-GO structure consisting of strongly defected fragments of graphene flakes (a) and more general scheme how the ruptured hole edges can serve as “pillars” for graphene scaffolds.

The structure of KOH activated material was cited in some previous publications simply as “activated graphene”. However, it is obvious from images shown in Fig. 2 that the samples need to be considered as three-dimensionally arranged irregular packing of strongly defected graphene layers (Fig. 6a). The powder of r-GO typically has very low bulk density with individual few layered graphene flakes not bound to each other. Annealing with KOH results in formation of solid micrometer size grains which consist of more densely packed and interconnected perforated graphene sheets. The role of pillaring units separating graphene sheets from each other could be played e.g. by ruptured edges of holes (Fig. 6b). The irregular shape of r-GO flakes and defects created by gasification prevents formation of graphitic structure.

The maximal SSA observed in our experiments was ~3400 m²/g, the SSA values over 3000 m²/g reproduced in at least 15 separately annealed samples. These values are comparable to the highest reported for nanostructured carbons, but still below 4000-5000 m²/g theoretically predicted for highly porous perforated ordered graphene multilayers which provides a promise for even further improved hydrogen storage of graphene scaffolds.¹⁶

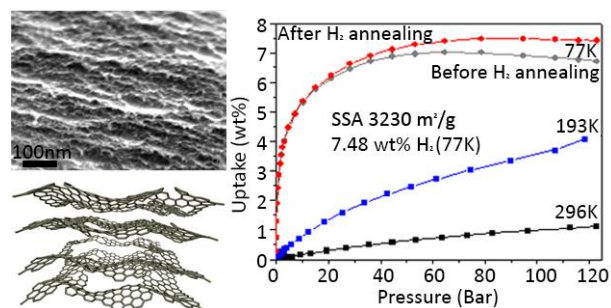
In conclusion, KOH activation of thermally exfoliated r-GO was tuned to produce samples with ultra-high BET surface area up to ~3400 m²/g and pore volume up to 2.2 cm³/g, superior to any other carbon materials. Furthermore, our graphene-based materials successfully compete with MOFs regarding the pore volume and hydrogen storage properties.^{22,23} As a result of activation treatment the r-GO are transformed into three-dimensional structure composed by strongly defected and interconnected graphene layers. Hydrogen storage parameters of graphene scaffolds produced by KOH activation measured for a-r-GO sample with ~3230 m²/g SSA after additional activation using high temperature annealing in hydrogen gas were 1.25 wt% at 293 K (120 bar), 1.61 wt% at 273 K (120 bar), 4.23 wt% (120 bar) at 193 K (temperature of solid CO₂) and ~7.48 wt% (saturation value) at 77 K.

Acknowledgement

This work was financially supported by the Swedish Research Council, Grant no. 621-2012-3654 (A.T) and by the Graphene Flagship (contract no. NECT-ICT-604391). We thank A. Shchukarev for help with XPS analysis.

Notes and references

1. K. Spyrou, D. Gournis and P. Rudolf, *Ecs J Solid State Sc*, 2013, **2**, M3160-M3169.
2. L. L. Zhang, X. Zhao, M. D. Stoller, Y. W. Zhu, H. X. Ji, S. Murali, Y. P. Wu, S. Perales, B. Clevenger and R. S. Ruoff, *Nano Lett*, 2012, **12**, 1806-1812.
3. L. Zhang, F. Zhang, X. Yang, G. K. Long, Y. P. Wu, T. F. Zhang, K. Leng, Y. Huang, Y. F. Ma, A. Yu and Y. S. Chen, *Sci Rep-Uk*, 2013, **3**.
4. J. C. Wang and S. Kaskel, *J Mater Chem*, 2012, **22**, 23710-23725.
5. M. A. de la Casa-Lillo, F. Lamari-Darkrim, D. Cazorla-Amoros and A. Linares-Solano, *J Phys Chem B*, 2002, **106**, 10930-10934.
6. M. Jorda-Beneyto, F. Suarez-Garcia, D. Lozano-Castello, D. Cazorla-Amoros and A. Linares-Solano, *Carbon*, 2007, **45**, 293-303.
7. N. P. Stadie, J. J. Vajo, R. W. Cumberland, A. A. Wilson, C. C. Ahn and B. Fultz, *Langmuir*, 2012, **28**, 10057-10063.
8. H. L. Wang, Q. M. Gao and J. Hu, *J Am Chem Soc*, 2009, **131**, 7016-7022.
9. G. Yushin, R. Dash, J. Jagiello, J. E. Fischer and Y. Gogotsi, *Adv Funct Mater*, 2006, **16**, 2288-2293.
10. G. Srinivas, Y. W. Zhu, R. Piner, N. Skipper, M. Ellerby and R. Ruoff, *Carbon*, 2010, **48**, 630-635.
11. Y. W. Zhu, S. Murali, M. D. Stoller, K. J. Ganesh, W. W. Cai, P. J. Ferreira, A. Pirkle, R. M. Wallace, K. A. Cychosz, M. Thommes, D. Su, E. A. Stach and R. S. Ruoff, *Science*, 2011, **332**, 1537-1541.
12. V. Tozzini and V. Pellegrini, *Phys Chem Chem Phys*, 2013, **15**, 80-89.
13. A. G. Klechikov, G. Mercier, P. Merino, S. Blanco, C. Merino and A. V. Talyzin, *Micropor Mesopor Mat*, 2015, **210**, 46-51.
14. K. R. Matranga, A. L. Myers and E. D. Glandt, *Chem Eng Sci*, 1992, **47**, 1569-1579.
15. I. A. Baburin, A. Klechikov, G. Mercier, A. V. Talyzin and G. Seifert, *International Journal of Hydrogen Energy*, 2015, **40**, 6594-6599.
16. H. Nishihara, P. X. Hou, L. X. Li, M. Ito, M. Uchiyama, T. Kaburagi, A. Ikura, J. Katamura, T. Kawarada, K. Mizuuchi and T. Kyotani, *J Phys Chem C*, 2009, **113**, 3189-3196.
17. A. V. Talyzin, T. Szabo, I. Dekany, F. Langenhorst, P. S. Sokolov and V. L. Solozhenko, *J Phys Chem C*, 2009, **113**, 11279-11284.
18. Z. Li, B. Song, Z. K. Wu, Z. Y. Lin, Y. G. Yao, K. S. Moon and C. P. Wong, *Nano Energy*, 2015, **11**, 711-718.
19. S. W. Wang, F. Tristan, D. Minami, T. Fujimori, R. Cruz-Silva, M. Terrones, K. Takeuchi, K. Teshima, F. Rodriguez-Reinoso, M. Endo and K. Kaneko, *Carbon*, 2014, **76**, 220-231.
20. B. Zheng, T. W. Chen, F. N. Xiao, W. J. Bao and X. H. Xia, *J Solid State Electr*, 2013, **17**, 1809-1814.
21. G. Srinivas, J. Burrell and T. Yildirim, *Energ Environ Sci*, 2012, **5**, 6453-6459.
22. I. Senkovska and S. Kaskel, *Chem Commun*, 2014, **50**, 7089-7098.
23. N. Klein, I. Senkovska, I. A. Baburin, R. Gruncker, U. Stoeck, M. Schlichtenmayer, B. Streppel, U. Mueller, S. Leoni, M. Hirscher and S. Kaskel, *Chem-Eur J*, 2011, **17**, 13007-13016.
24. B. Schmitz, U. Muller, N. Trukhan, M. Schubert, G. Ferey and M. Hirscher, *Chemphyschem*, 2008, **9**, 2181-2184.
25. B. Assfour, S. Leoni, G. Seifert and I. A. Baburin, *Adv Mater*, 2011, **23**, 1237-1241.
26. M. Hirscher and M. Becher, *J Nanosci Nanotechno*, 2003, **3**, 3-17.
27. B. Panella, M. Hirscher and S. Roth, *Carbon*, 2005, **43**, 2209-2214.
28. A. Ghosh, K. S. Subrahmanyam, K. S. Krishna, S. Datta, A. Govindaraj, S. K. Pati and C. N. R. Rao, *J Phys Chem C*, 2008, **112**, 15704-15707.
29. C. C. Huang, N. W. Pu, C. A. Wang, J. C. Huang, Y. Sung and M. D. Ger, *Sep Purif Technol*, 2011, **82**, 210-215.
30. E. Poirier, R. Chahine and T. K. Bose, *Int J Hydrogen Energy*, 2001, **26**, 831-835.

Figure for Table of Content.**Text for Table of Content entry.**

Graphene scaffold material with surface area of $\sim 3300 \text{ m}^2/\text{g}$ showed hydrogen uptakes up to $\sim 7.5 \text{ wt}\%$ at 77K.